Optics Letters

Ultrafast laser-absorption spectroscopy for single-shot, mid-infrared measurements of temperature, CO, and CH₄ in flames

RYAN J. TANCIN,^{1,*} ZIQIAO CHANG,² MINGMING GU,² VISHNU RADHAKRISHNA,² ROBERT P. LUCHT,² AND CHRISTOPHER S. GOLDENSTEIN²

¹School of Aeronautics and Astronautics, Purdue University, 585 Purdue Mall, West Lafayette, Indiana 47907, USA ²School of Mechanical Engineering, Purdue University, 585 Purdue Mall, West Lafayette, Indiana 47907, USA *Corresponding author: rtancin@purdue.edu

Received 14 October 2019; revised 15 November 2019; accepted 18 November 2019; posted 19 November 2019 (Doc. ID 380091); published 14 January 2020

This Letter describes the development of an ultrafast (i.e., femtosecond), mid-infrared (mid-IR), laser-absorption diagnostic and its initial application to measuring temperature, CO, and CH₄ in flames. The diagnostic employs a Ti:sapphire oscillator emitting 55 fs pulses near 800 nm that were amplified and converted into the mid-IR though optical parametric amplification at a repetition rate of 5 kHz. The pulses were directed through the test gas and into a high-speed mid-IR spectrograph to image spectra across a ≈30 nm bandwidth with a spectral resolution of ≈0.3 nm. Gas properties were determined by least-squares fitting simulated absorbance spectra to measured single-shot absorbance spectra. The diagnostic was validated with measurements of temperature, CO, and CH₄ in a static-gas cell with an accuracy of 0.7% to 1.8% of known values. Singleshot, 5 kHz measurements of temperature and CO column density were acquired near 4.9 µm in a laser-ignited HMX (i.e., 1,3,5,7-tetranitro-1,3,5,7-tetrazoctane) flame and exhibited $1 - \sigma$ precisions of 0.4% and 2.3%, respectively, at ≈2700 K. Further, temperature and CH₄ column density measurements were acquired near 3.3 µm in a partially premixed CH₄-air flame produced by a Hencken burner and exhibited $1 - \sigma$ precisions of 0.3% and 1% respectively, at ≈1000 K. © 2020 Optical Society of America

https://doi.org/10.1364/OL.45.000583

Laser-absorption spectroscopy (LAS) is a powerful technique for providing noninvasive, quantitative measurements of temperature and species concentrations in combustion environments [1]. LAS diagnostics often employ narrowband, wavelength-tunable lasers (e.g., tunable diode lasers, quantum-cascade lasers) that are capable of measuring gas conditions via spectra measured over several cm⁻¹ at rates up to 1 MHz [1,2]. While highly useful, the narrowband nature of this approach can: (1) limit the dynamic range of such diagnostics [3], (2) complicate measurements of molecules with broad spectra (e.g., at high pressures), and (3) often prevent multispecies measurements using a single light source. To address these issues,

numerous researchers have developed broadband LAS diagnostics, typically with 10s to 1000s of cm⁻¹ of spectral bandwidth [4–11].

One common broadband LAS technique employs scannedwavelength lasers with broad wavelength-tuning capabilities. For example, Sanders et al. [4] used a vertical-cavity surfaceemitting laser (VCSEL) to scan ≈30 cm⁻¹ near 760 nm in order to acquire measurements of temperature and O2 at 500 Hz in high-pressure gases. More recently, a microelectricalmechanical-systems (MEMS) VCSEL capable of tuning \approx 170 cm⁻¹ near 1.4 μ m has been used to measure temperature and H₂O at 100 kHz in a wide variety of combustion applications (see [5] and references therein). In addition, external-cavity quantum-cascade lasers in the mid-and far-IR with large-amplitude (≈100 cm⁻¹) tuning have emerged, which recently enabled measurements of C_2H_4 between 8.5 μm and 11.7 µm in shock-heated gases with a time resolution of 3 ms [6]. Unfortunately, light sources suitable for this approach are limited to only a few wavelength regions, and the time resolution is limited to the reciprocal of the scan frequency (typically on the order of 1 ms to 10 μ s).

Numerous techniques employing ultrafast lasers (i.e., lasers emitting ultrashort, typically <10 ps, pulses) have also been used for broadband LAS measurements of combustion gases; however, they have not been applied in the mid-infrared (mid-IR). For example, Sanders [7] used a femtosecond-fiberlaser-pumped supercontinuum source and a scanning bandpass filter to produce 1000 cm⁻¹ of bandwidth near 1450 nm for measurements of temperature and several species (H₂O, CO₂, C₂H₂, C₂H₆O) at 50 kHz. More recently, Blume and Wagner [8] used a commercial supercontinuum lightsource with a dispersing fiber to acquire measurements of CH₄ and temperature at 200 Hz using 110 cm⁻¹ of bandwidth near 1650 nm. One drawback to this approach is the relatively large noise levels inherent to supercontinuum lightsources, which has prevented single-shot measurements. Recently, Draper et al. [10] applied a dual-frequency-comb spectrometer to characterize combustion environments. The authors used 160 cm⁻¹ of bandwidth near 1655 nm to measure temperature and CH₄ concentration in

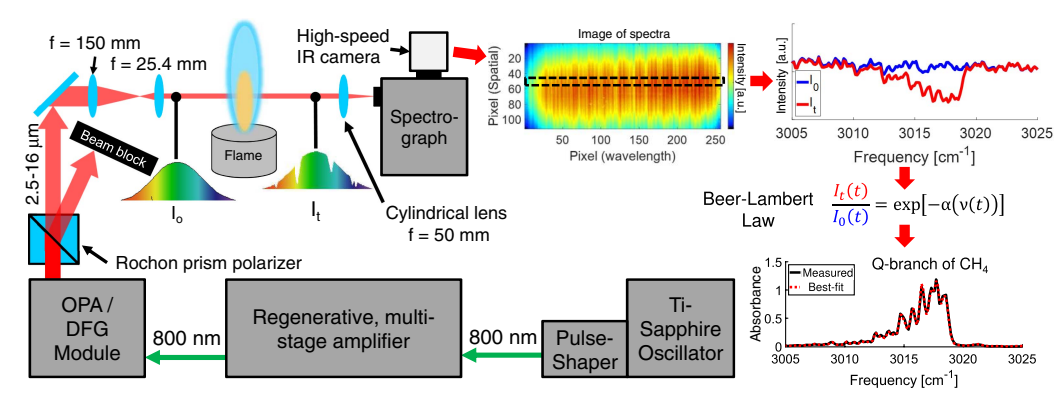


Fig. 1. Concept schematic illustrating the experimental setup and data processing steps employed by the ultrafast-laser-absorption diagnostic.

a rapid compression machine. Currently, multishot averaging and filtering have extended the repetition rate to $\approx\!1.4~\mathrm{kHz}$ [10]. Most recently, time-resolved, optically gated absorption (TOGA) spectroscopy was developed by Stauffer *et al.* [11] to provide background-free measurements of absorption spectra. The authors used an amplified Ti:sapphire laser and two frequency-doubling processes to produce pulses centered near 310 nm with over 300 $~\mathrm{cm}^{-1}$ of bandwidth to acquire spectra of OH with 10 ps time resolution.

Here we demonstrate the first, to our knowledge, ultrafast, single-shot, mid-IR LAS diagnostic for temperature and species measurements in combustion gases. In addition to the aforementioned potential advantages of broadband LAS diagnostics (e.g., improved high-pressure capability, high-dynamic range, multispecies measurements), we demonstrate that this diagnostic offers several unique advantages: (1) ultrafast (<1 ps) time resolution, (2) access to strong fundamental absorption bands located throughout the midwave IR using a single light source and camera, and (3) potential for single-shot, spatially resolved (1D) thermometry and species measurements at 5 kHz. This Letter describes the design and operating principles of this diagnostic technique, in addition to its initial validation and application to characterizing flames.

The experimental system and data processing procedures are summarized in Fig. 1. Ultrafast laser pulses were generated by a mode-locked Ti:sapphire laser (Coherent Mantis) at a rate of 80 MHz and a center wavelength near 800 nm. The pulses were tailored by a Femtojock pulse-shaper to prepare them for amplification by a multistage regenerative chirped-pulse amplifier (Coherent Legend Elite Duo). The amplifier produced pulses with a pulse energy of 2 mJ and duration of 55 fs at a repetition rate of 5 kHz. Next, the pulses were directed into an optical parametric amplifier module (Coherent OPerA Solo) equipped with noncollinear difference-frequency generation (NDFG) crystals to generate ultrashort mid-IR pulses. The mid-IR pulses contain ≈600 cm⁻¹ of useful spectral bandwidth, and the center wavelength can be tuned between 2.5 µm and 18 µm via computer-controlled manipulation of the crystals. For the results presented here, the pulse energies were 30 µJ and 4 µJ for wavelengths near 3315 nm and 4858 nm, respectively. A MgF₂ Rochon prism polarizer was used to attenuate the pulse energy to $\approx 0.75 \mu J$ to prevent camera saturation. Next, the mid-IR pulses were directed through the test gas and then focused onto the slit of an Andor Shamrock 500i imaging spectrometer using

a cylindrical lens (ZnSe, 50 mm focal length). A 300 groove/mm diffraction grating was used to spectrally disperse the pulses, and a Telops FAST-IR 2k high-speed IR camera was used to image each individual pulse in 2D. This configuration provided a theoretical spectral resolution and bandwidth of 0.21 nm and 38 nm, respectively, and similar metrics were achieved in practice. The IR camera recorded 52×256 pixels with a 5 μ s exposure time at 10 k frames-per-second in order to record two images per pulse (one for the pulse, another to image flame and ambient emission between pulses so it could be subtracted off in postprocessing). The camera was synchronized with the laser output.

CO and CH₄ were chosen for the initial application of this diagnostic primarily to demonstrate its ability to measure gas properties via molecules with well isolated lines (CO) or blended spectra (CH₄). Measurements were acquired in CO's P-branch near 2060 cm⁻¹ due to favorable absorbance levels, lack of interference from other combustion relevant species (e.g., H₂O, CO₂), and previous combustion studies demonstrating the utility of this spectral region [12–15]. Temperature and CH₄ measurements were acquired via CH₄'s Q-branch near 3015 cm⁻¹ due to its strength, isolation from interfering absorption lines, and the large number of transitions with unique lower-state energy comprising it that enhances temperature sensitivity [1,3].

The center wavelength of the spectrograph and light source were set to 4858 nm for measurements of temperature and CO concentration. Measurements were acquired in a staticgas cell [16] (9.4 cm path length) filled with a commercially prepared gas mixture (2% CO, 1.8% CO₂, and 96.2% N₂ by mole) at 1 atm and 296 K to validate the accuracy of the diagnostic and data processing routine. Measurements of temperature and CO column density ($\chi_{CO}L$) were also acquired in a laser-ignited HMX flame [see Fig. 2(a)]. The HMX was pressed into a 6 mm diameter, 3 mm tall cylindrical pellet and ignited with a CO₂ laser emitting 78 W/cm² at a wavelength of 10.6 μ m for the entire test duration. For this test, the $1/e^2$ diameter of the ultrafast beam was reduced from 7.9 mm to 1.4 mm via a lens telescope consisting of a CaF₂ plano-convex lens (f = 150 mm) and an AR-coated Si plano-convex lens (f = 25.4 mm). The measurement was acquired 7.5 mm above the initial surface location of the pellet.

The accuracy of the temperature and CH₄ diagnostic was also validated via measurements in a static-gas cell (0.7 cm path

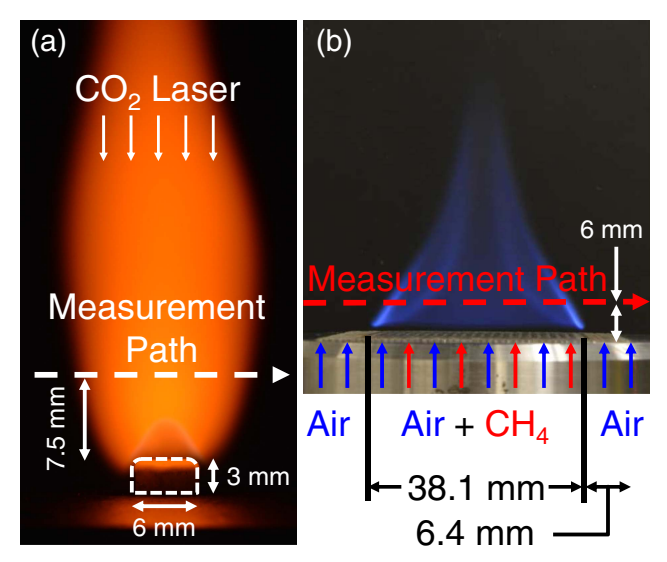


Fig. 2. Images of and pertinent dimensions for the (a) laser-ignited HMX flame and (b) partially premixed CH_4 -air flame studied here.

length) and Fig. 1 illustrates an example single-shot measurement of CH₄'s Q-branch at 296 K and 1 atm. The cell was filled with a commercially prepared mixture of 7% CH₄, 15% C₂H₂, and 78% N₂ by mole at 1 atm and 296 K. Measurements were also acquired in a laminar, partially premixed CH₄-air flame [see Fig. 2(b)]. The flame was produced by a Hencken burner with a 38.1 mm square core consisting of a honeycomb of alternating jets of CH₄ and air surrounded by a 6.4 mm thick coflow of air. The equivalence ratio was 6.4 with an exit plane velocity of \approx 0.9 cm/s.

For each experiment, the measured spectral absorbance (α) was calculated at each frequency (ν) using the measured incident (I_o) and transmitted (I_t) laser intensity and Beer's Law: $\alpha(\nu) = -\ln[I_t(\nu)/I_o(\nu)]$. I_o was obtained empirically by recording and averaging (to reduce noise) 200 images of ultrashort mid-IR pulses in the absence of the test gas. The signal-to-noise ratio (SNR) of I_o was then further increased by averaging 8 to 18 (depending on test) spectra of I_o (acquired by adjacent rows of pixels within a single image) together. For the results reported here, this corresponds to spatial averaging across less than 1 mm (vertically) at the measurement location in the flame gas.

The gas temperature and absorbing-species concentration were determined by least-squares fitting simulated absorbance

spectra to the measured absorbance spectra. The fitting routine employs the following free parameters: temperature, absorbing species concentration, a frequency shift, the width of the empirical instrument response function (IRF), and a scaling factor for I_{ϱ} to account for shot-to-shot fluctuations in pulse energy. The frequency axis of the data was determined by matching three to four prominent absorption features to their linecenter frequencies (provided by a spectroscopic database) and fitting a linear frequency axis to those points. Absorbance spectra were simulated in the fitting routine using the following procedure. (1) A high-resolution (≈ 0.0005 cm⁻¹) absorbance spectrum was simulated using $\alpha_{HR}(v) = \sum_{j} S_{j}(T)\phi_{j}(v) P \chi L$ and a spectroscopic database where S_j and ϕ_j are the linestrength and lineshape of transition j, respectively, T is the gas temperature, P is the gas pressure, χ is the absorbing species mole fraction, and L is the path length through the absorbing gas. Transition lineshapes were modeled as a Voigt profile. (2) The resolution of the empirical baseline (i.e., I_0) was increased to match that of $\alpha_{\rm HR}$ via linear interpolation, thereby yielding $I_{o,{\rm HR}}$. (3) Next, Eq. (1) was used to produce a high-resolution, semiempirical transmission spectrum ($I_{t,HR,conv}$), which has been convolved with the IRF of the spectrograph-camera setup. (4) $I_{o,HR}$ was then convolved with the IRF to yield $I_{\theta, HR, conv}$. (5) A simulated absorbance spectrum with the IRF accounted for was then calculated from $I_{\theta, HR, conv}$ and $I_{t, HR, conv}$ using Beer's Law and then downsampled to the same frequency axis as the measured absorbance spectrum to enable direct comparison and the sumof-squared error (the optimization parameter) to be computed by the fitting routine. Equation (1) is as follows:

$$I_{t,\mathrm{HR,conv}}(\lambda) = \int_{-\infty}^{\infty} \mathrm{IRF}(\lambda - \tau) I_{\theta,\mathrm{HR}}(\tau) e^{-\alpha_{\mathrm{HR}}(T,P,\chi,L)} \mathrm{d}\tau. \tag{1}$$

Here, λ is the wavelength, and τ is the convolution shift variable. The IRF was modeled as a Lorentzian lineshape.

It is important to note that the IRF is not directly convolved with the simulated absorbance spectrum because the spectrograph-camera setup "sees" a transmission spectrum, not an absorbance spectrum. The convolution with the IRF was executed in wavelength-space where the full width at half-maximum (FWHM) of the IRF is constant. The spectroscopic model for CO employed the HITEMP 2019 database [17], and the spectroscopic model for CH₄ utilized a preliminary version (yet to be openly released) of the HITEMP 2019 database for methane [17] that is based on work by Rey *et al.* [18].

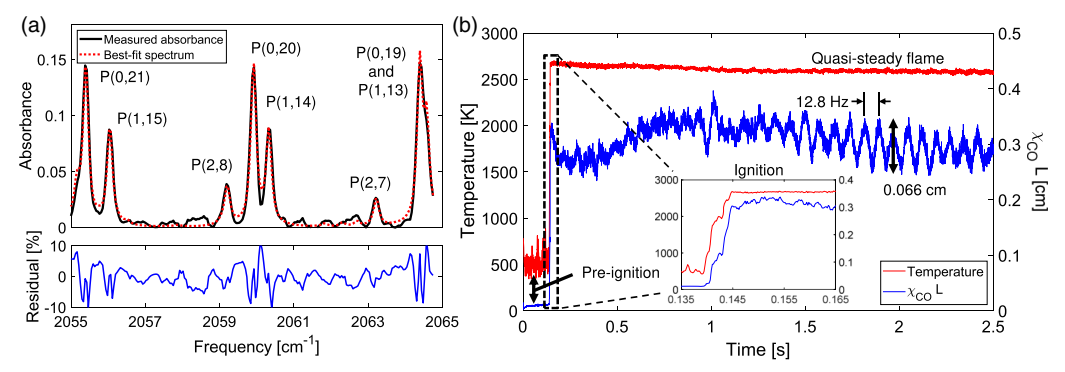


Fig. 3. Example (a) single-shot measurement and best-fit spectrum for CO near 4.9 μ m and (b) corresponding time history of temperature and $\chi_{CO}L$ acquired in a laser-ignited HMX flame.

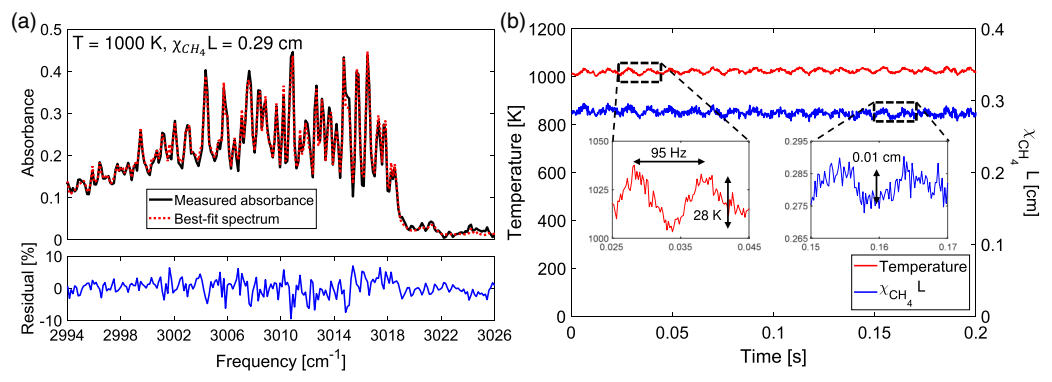


Fig. 4. Example (a) single-shot measurement and best-fit spectrum of CH_4 's Q-branch and (b) corresponding time history of temperature and $\chi_{CH_4}L$ acquired in partially premixed CH_4 -air flame.

Measurements of temperature and CO concentration in static-gas-cell experiments were accurate within 1.5% and 1.8% of known values, respectively, with a $1 - \sigma$ precision of 0.7% and 1.2%, respectively. Figure 3(a) displays representative measured and best-fit absorbance spectra acquired in the HMX flame while at quasi-steady-state. The $1-\sigma$ noise level in the measured absorbance was 0.25%. Time histories of temperature and $\chi_{CO}L$ are shown in Fig. 3(b). The diagnostic resolved preignition decomposition of HMX through quasi-steady burning. At the quasi-steady-state, the measured time-averaged temperature and CO column density were 2620 K and 0.32 cm (i.e., 21.3% by mole for a 1.5 cm thick flame), respectively, which agrees well with measurements acquired in our lab using quantum-cascade lasers similar to as reported in [14]. The $1-\sigma$ precisions are 10 K (0.4%) and 0.007 cm (2.3%). Throughout the burn, the temperature decreased by \approx 100 K due to the surface of HMX regressing away from the measurement line-of-sight. Large amplitude oscillations in $\chi_{CO}L$ are observed at 12.8 Hz as a result of a natural flame instability [19]. Temperature measurements acquired prior to ignition were enabled by the broad spectral bandwidth of the measurement. Measurements with an absorbance SNR as low as 20 were made, occurring at a CO column density of 0.003 cm and temperature of 500 K.

The temperature and CH₄ concentration measured in static-gas-cell experiments were accurate within 1.2% and 0.8% of known values, respectively, with a $1-\sigma$ precision of 0.2% and 0.7%, respectively. Figure 4(a) shows typical single-shot absorbance spectra of CH₄'s *Q*-branch, and Fig. 4(b) shows measured time histories of temperature and CH₄ column density acquired in a partially premixed CH₄-air Hencken-burner flame. The time-averaged values of temperature and column density are 1023 K and 0.283 cm, both of which exhibit a 95 Hz oscillation (due to a combustion instability) with a peak-to-peak amplitude of 28 K and 0.01 cm, respectively. After accounting for this oscillation, the $1-\sigma$ precision of the measured temperature and column density are 3 K (0.3%) and 0.003 cm (1%), respectively. The results shown were acquired with an absorbance-noise level of \approx 0.5%.

The results presented in this Letter illustrate that ultrafast laser-absorption spectroscopy in the mid-IR is capable of high-fidelity characterization of combustion gases with sub-picosecond time resolution. **Funding.** Air Force Office of Scientific Research (FA9550-18-1-0210); NSF CBET (1834972).

Acknowledgment. The authors thank Austin McDonald for advice regarding the development of the spectral-fitting routine and Dr. Robert Hargreaves for sharing a preliminary version of the HITEMP 2019 database for CH₄.

Disclosures. The authors declare no conflicts of interest.

REFERENCES

- C. S. Goldenstein, R. M. Spearrin, J. B. Jeffries, and R. K. Hanson, Prog. Energy Combust. Sci. 60, 132 (2017).
- D. I. Pineda, F. A. Bendana, K. K. Schwarm, and R. M. Spearrin, Combust. Flame 207, 379 (2019).
- X. An, A. W. Caswell, and S. T. Sanders, J. Quant. Spectrosc. Radiat. Transfer 112, 779 (2011).
- S. T. Sanders, J. Wang, J. B. Jeffries, and R. K. Hanson, Appl. Opt. 40, 4404 (2001).
- K. D. Rein, S. Roy, S. T. Sanders, A. W. Caswell, F. R. Schauer, and J. R. Gord, Appl. Phys. B 123, 88 (2017).
- C. L. Strand, Y. Ding, S. E. Johnson, and R. K. Hanson, J. Quant. Spectrosc. Radiat. Transfer 222-223, 122 (2019).
- 7. S. T. Sanders, Appl. Phys. B 75, 799 (2002).
- 8. N. Göran Blume and S. Wagner, Opt. Lett. 40, 3141 (2015).
- P. J. Schroeder, R. J. Wright, S. Coburn, B. Sodergren, K. C. Cossel, S. Droste, G. W. Truong, E. Baumann, F. R. Giorgetta, I. Coddington, N. R. Newbury, and G. B. Rieker, Proc. Combust. Inst. 36, 4565 (2017)
- A. D. Draper, R. K. Cole, A. S. Makowiecki, A. Zdanawicz, J. Mohr, A. Marchese, N. Hoghoogi, and G. B. Rieker, Opt. Express 27, 10814 (2019)
- H. U. Stauffer, P. S. Walsh, S. Roy, and J. R. Gord, AIAA Scitech 2019 Forum (2019), p. 1607.
- R. M. Spearrin, C. S. Goldenstein, I. A. Schultz, J. B. Jeffries, and R. K. Hanson, Appl. Phys. B 117, 689 (2014).
- D. D. Lee, F. A. Bendana, S. A. Schumaker, and R. M. Spearrin, Appl. Phys. B 124, 77 (2018).
- R. J. Tancin, G. C. Mathews, and C. S. Goldenstein, Rev. Sci. Instrum. 90, 045111 (2019).
- R. J. Tancin, R. M. Spearrin, and C. S. Goldenstein, Opt. Express 27, 14184 (2019).
- K. K. Schwarm, H. Q. Dinh, C. S. Goldenstein, D. I. Pineda, and R. M. Spearrin, J. Quant. Spectrosc. Radiat. Transfer 227, 145 (2019).
- R. J. Hargreaves, I. E. Gordon, R. V. Kochanov, and L. S. Rothman, *EPSC-DPS Joint Meeting* (2019), 13, p. 919-1.
- 18. M. Rey, A. V. Nikitin, and V. G. Tyuterev, Astrophys. J. 847, 105 (2017).
- J. C. Finlinson, T. Parr, and D. Hanson-Parr, Symp. (Int.) Combust. 25, 1645 (1994).